TUD-C-Supported Tungsten Oxide-Doped Titania Catalysts for Cyclohexane Oxidation

Chui Min Ling[1], Leny Yuliati[2], Hendrik Oktendy Lintang[2] and Siew Ling Lee[1, 3*]
[1]Department of Chemistry, Faculty of Science, Universiti Teknologi Malaysia, 81310 Johor Bahru, Johor, Malaysia.
[2]Ma Chung Research Center for Photosynthetic Pigments, Universitas Ma Chung, Villa Puncak Tidar N-01, Malang 65151, Indonesia.
[3]Center for Sustainable Nanomaterials, Ibnu Sina Institute for Scientific and Industrial Research, Universiti Teknologi Malaysia, 81310 Johor Bahru, Johor, Malaysia.
*Corresponding author: (e-mail: sllee@ibnusina.utm.my)

A new oxidation catalyst of Technische Universiteit Delft-Crystalline (TUD-C)-supported tungsten oxide-doped titania (WO_3-TiO_2/TUD-C) has been successfully synthesized. WO_3-modified TiO_2 was reported as a potential oxidation catalyst. However, the low surface area and porosity have restricted the catalytic performance of this material. In order to overcome this problem, a mesoprorous zeolitic compound of TUD-C was used as a catalyst support for WO_3-TiO_2 in this work. The TUD-C-supported 1 mol% WO_3-TiO_2 was synthesized by adding pre-synthesized WO_3-TiO_2 onto the TUD-C support. Both X-ray diffractometry and Fourier transform infrared analyses indicated MFI zeolitic framework formation in the TUD-C-supported 1 mol% WO_3-TiO_2. Both surface area and porosity of the resulting WO_3-TiO_2/TUD-C were significantly higher than those of bare WO_3-TiO_2. The catalytic performance of the resulting materials was evaluated through cyclohexane oxidation at 70^{o}C for 4 hours. It has been demonstrated that the catalytic activity of WO_3-TiO_2 increased approximately 2-fold after loading on TUD-C support.

Key words: TUD-C; titania; cyclohexane oxidation; tungsten oxide

Received: October 2019; Accepted: February 2020

Cyclohexane is an important hydrocarbon with saturated cyclic alkane group which is principally applied in the production of intermediates and fine chemicals. In addition, cyclohexane is mainly utilized for the fine chemical manufacturing for the production of assorted materials, such as solvents, herbicides, plasticizers etc. [1]. Most of the cyclohexane is predominantly consumed in the production of Ketone-Alcohol oil (K-A oil), which are cyclohexanol and cyclohexanone. K-A oil is commonly employed for the manufacture of fine chemicals, for instance caprolactam, adipic acid, and other materials such as pharmaceutical coating dye. Oxidation of cyclohexane generally produces adipic acid and caprolactam for the polymer and nylon production [2].

For the production of K-A oil, oxidation of cyclohexane is needed in the manufacturing of polymer and nylon. However, cyclohexane oxidation would generate minimal K-A oil conversion, rigid environmental pollution, and enormous utilization of energy with the presence of homogeneous catalysts under extremely high temperature and pressure [3]. As a result, heterogeneous catalysts can be promising catalysts for cyclohexane oxidation under benevolent conditions. For the last two decades, titania (TiO_2) and TiO_2-based heterogeneous catalysts have been studied for the cyclohexane oxidation [4-6].

In fact, TiO_2 catalysts have been widely applied in pollutant removal, wastewater treatment, and fine chemical manufacturing. However, TiO_2 is less efficacious due to its limited active sites. Therefore, some efforts were reported to enhance properties of TiO_2 catalysts with metal doping including Nb, V, and W [7-10]. It was reported previously that WO_3-modified TiO_2 was a better catalyst for SO_2 oxidation as compared to bare TiO_2 due to existence of more surface redox sites upon addition of WO_3 [11]. On the other hand, the inadequate surface area of TiO_2 influenced the performance of catalytic and photocatalytic activities because the agglomeration and aggregation of TiO_2 restricted the number of active sites for substances and substrates [12]. To overcome this problem, TiO_2 or metal oxide-modified TiO_2 catalysts have to be supported onto a high surface area material [13, 14].

Technische Universiteit Delft-Crystalline (TUD-C) is a relative new mesoporous support. It has three dimensional and sponge-like pore structure, high surface area, and well-distributed pore size [15]. In addition, TUD-C materials can be synthesized efficiently without any surfactants and thus environmentally safe [16]. TUD-C materials as catalyst support would be further explored since the report on the application of TUD-C is inadequate.

In this work, we developed new WO_3-TiO_2 supported on TUD-C oxidative catalysts. The physiochemical properties of TUD-C-supported 1 mol% tungsten oxide-doped titania were studied. Furthermore, the catalytic performance of TUD-C-supported 1 mol% tungsten oxide-doped titania in cyclohexane oxidation was investigated.

EXPERIMENTAL

1. Preparation of Catalysts

Four catalysts: TiO_2, TUD-C, WO_3-TiO_2, and WO_3-TiO_2/TUD-C were synthesized. WO_3-TiO_2/TUD-C catalysts were prepared via the sol-gel method, followed by wet-impregnation, hydrothermal treatment, and calcination. All the materials were synthesized using chemicals without further purification.

1.1. Synthesis of TiO_2

TiO_2 was synthesized through the sol-gel method. Titanium tetraisopropoxide (TTIP), ethanol as solvent, and acetylacetone as chelating agent were mixed according to the molar composition of 1: 100:2 [17]. The mixture was mixed for 2 hours and then evaporated at 80°C. The sample was dried overnight at 110°C and calcined at 500°C to obtain the TiO_2.

1.2. Synthesis of WO_3-TiO_2

Tungsten oxide-doped titania, WO_3-TiO_2 was synthesized through the sol-gel method. TTIP was mixed with ethanol as solvent and acetylacetone as chelating agent according to the molar composition of 1: 100: 2. Ammonium tungstate was the respective tungsten oxide salt, as the precursor of tungsten for the production of the tungsten oxide-doped TiO_2. Meanwhile, 1 mol% of ammonium tungstate was dissolved in 2 mL of distilled water. The mixture was mixed for 2 hours and then evaporated at 80°C. The sample was dried overnight at 110°C and calcined at 500°C to obtain the tungsten oxide-doped TiO_2 (WO_3/TiO_2).

1.3. Synthesis of TUD-C and WO_3-TiO_2/TUD-C

TUD-C was prepared by stirring triethanolamine (TEA), distilled water, tetraethyl orthosilicate (TEOS), and Zeolite Socony Mobil-5 (ZSM-5) for the homogeneous synthesis of TUD-C [18]. Next, tetraethylammonium hydroxide (TEAOH) was added dropwise into the mixture. The molar composition for the synthesis of TUD-C was 1 TEOS : 0.1 Al_2O_3 : 0.5 TEA : 0.1 TEAOH. The TUD-C material was synthesized with the Si/Al molar ratio of 30. The mixture was stirred at ambient temperature for 2 hours. After that, the mixture was evaporated at ambient temperature for 24 hours. Then, the mixture was solidified after aging and a solid gel was formed and ground to incur fine powder. The sample was treated hydrothermally at 130°C for 10 hours. After the hydrothermal treatment, the sample was dried at 130°C and then calcined at 800°C for 6 hours to eliminate the organic compounds in the sample. For WO_3-TiO_2/TUD-C, the pre-synthesized WO_3-TiO_2 was mixed with TEOS before the addition of TEA and distilled water and then TEAOH through wet impregnation. The weight ratio of WO_3/TiO_2: TUD-C was fixed at 1:30.

2. Material Characterizations

The materials synthesized were characterized by the powder X-ray diffraction (XRD) for the crystallinity identification and phase determination. The XRD analysis was performed on a powder Bruker Advance D8 diffractometer equipped with incident beam CuK_α monochromator. The crystallite size of TiO_2 was calculated using Scherrer equation shown in Equation (1) according to the peaks in the XRD pattern.

$$t = \frac{K\lambda}{\beta \cos\theta} \quad \text{Eq (1)}$$

Where, t is the crystalline size in nm, whereas K represents the dimensionless shape factor. λ is the X-ray wavelength, β is the full width at half maximum (FWHM) at 2θ, and θ indicates the Bragg's angle. The materials were analyzed using Fourier Transform Infrared (FT-IR) spectroscopy with the model Nicolet iS10 spectrometer equipped with Attenuated Total Reflectance (ATR) and diamond-crystal cell for the surface characterization. The diffuse-reflectance UV-Vis spectroscopy was performed using Perkin Elmer Ultraviolet-visible Spectrometer Lambda 900 to investigate the species of Ti for the materials. Quantachrome Surface Autosorb-6B sorption analyzer was used for the measurement of surface area and pore volume of the materials. Brunauer-Emmett-Teller (BET) theory was used for the surface area determination.

3. Catalytic Activity Testing

The catalytic testing was modified based a previous work [19]. The synthesized samples (150 mg), 2 g of cyclohexane (Analytical Reagent grade), and 20 mL of acetic acid were added one by one into a 3-necked round bottom flask with a reflux condenser and thermometer. Next, aqueous 30% H_2O_2 solution was added dropwise into the mixture. The mixture was stirred at 70°C for 4 hours. The mixture was filtered and extracted by diethyl ether twice. Excess water in the extracted organic phase was removed by using anhydrous $MgSO_4$. The products obtained were identified using gas chromatography equipped with mass spectroscopy. The cyclohexane conversion was calculated using Equation (2).

$$\text{Cyclohexane conversion (\%)} = \frac{C_0 - C_f}{C_0} \times 100 \qquad \text{Eq (2)}$$

Where, C_0 and C_f are initial concentration and final concentration, respectively.

RESULT AND DISCUSSIONS

1. Structure and Morphology Characterization

TiO_2, WO_3-TiO_2, TUD-C, and WO_3-TiO_2/TUD-C catalysts were synthesized adopting a sequence of combinatorial chemical synthesis methods including wet impregnation, sol-gel method, hydrothermal practice, and calcination approach. Figure 1 illustrates the XRD patterns of the pure TiO_2, WO_3-TiO_2, TUD-C, and WO_3-TiO_2/TUD-C. As evidenced, undoped TiO_2 was purely anatase and body-centerd tetragonal in shape (JCPDS 21-1272). Pure anatase of TiO_2 was obtained by Koh *et al*. [8] by using the sol-gel method. After doping of 1 mol% WO_3, WO_3-TiO_2 showed peaks which corresponded to anatase, implying TiO_2 anatase phase remained. Meanwhile, small peaks at $2\theta = 34^o$, 42^o, and 51^o were indicative of monoclinic WO_3 (JCPDS 43-1035), indicating the presence of crystalline WO_3 in the samples. For TUD-C, there were 2 sharp peaks at $2\theta = 8^o$ to 10° which corresponded to (101) and (200), indicating MFI zeolitic framework formation in the amorphous silica [20]. Detection of some peaks at $2\theta = 20^o$ to 25° was a good indication of aluminium silicate and ZSM-5 zeolite. Apparently, the MFI zeolitic framework was found in WO_3-TiO_2-supported TUD-C, suggesting successfully loading of WO_3-TiO_2 into TUD-C. Besides, anatase was detected in WO_3-TiO_2/TUD-C. However, WO_3 phase was not observed. It could be due to low amount of WO_3 in the material.

As expected, the crystallinity of WO_3-TiO_2 slightly decreased after loading into TUD-C mesoporous material. The crystalline size of all the materials was calculated using Scherrer equation and the results are tabulated in Table 1. The crystallite size of TiO_2 was 20 nm. After doping of WO_3 onto TiO_2, the crystallite size of WO_3-TiO_2 decreased. However, the crystallite size of WO_3-TiO_2/TUD-C was larger than those of TiO_2 and WO_3-TiO_2. The phenomenon could be explained by the successful incorporation of WO_3-TiO_2 into the framework of TUD-C [21].

Table 1 illustrates the BET surface area of TiO_2, WO_3-TiO_2, TUD-C, and WO_3-TiO_2/TUD-C. The surface area of TiO_2 was 21 m^2/g. The value was comparable to that of a previous report [8]. The surface area of WO_3-TiO_2 (17 m^2/g) was slightly lower than that of TiO_2. This could be due to possible displacement of WO_3 into interstitial space of TiO_2. As shown, the surface area of WO_3-TiO_2/TUD-C was 84 m^2/g, which was approximately 5 times higher than that of unsupported WO_3-TiO_2. The observation strongly suggested that usage of TUD-C as the support for WO_3-TiO_2 has remarkably increased the surface area of the resulting material. A similar finding was reported previously for Mo-TiO_2 supported on TUD-C support [21].

The porosity data including pore volume and pore radius of all the materials are listed in Table 1. The pore volume of WO_3-TiO_2 (0.07 cm^3/g) was lesser compared to TiO_2 (0.11 cm^3/g). Among the materials, TUD-C possessed the highest pore volume (0.30 cm^3/g) since it was a mesoporous material. It was not surprising that WO_3-TiO_2/TUD-C had lower pore volume (0.17 cm^3/g) than that of TUD-C. The phenomenon could be explained by dispersion of WO_3-TiO_2 particles on the pore wall of TUD-C. On the other hand, it was observed that the pore radius of WO_3-TiO_2 (1.95 nm) decreased after the loading on TUD-C where the pore radius of WO_3-TiO_2/TUD-C was only 0.92 nm. It could be due to accretion of WO_3-TiO_2 on the pore month of TUD-C, resulting in reduction of pore radius [20].

Table 1. Surface area, crystalline size, pore volume, and pore radius of the materials

Samples	Crystalline size (nm)	Surface area (m^2/g)	Pore volume (cm^3/g)	Pore radius (nm)
TiO_2	20	21	0.11	1.94
WO_3-TiO_2	17	15	0.07	1.95
TUD-C*	35	1451	0.30	0.92
WO_3-TiO_2/TUD-C	24	84	0.17	0.92

* Adapted from [20]

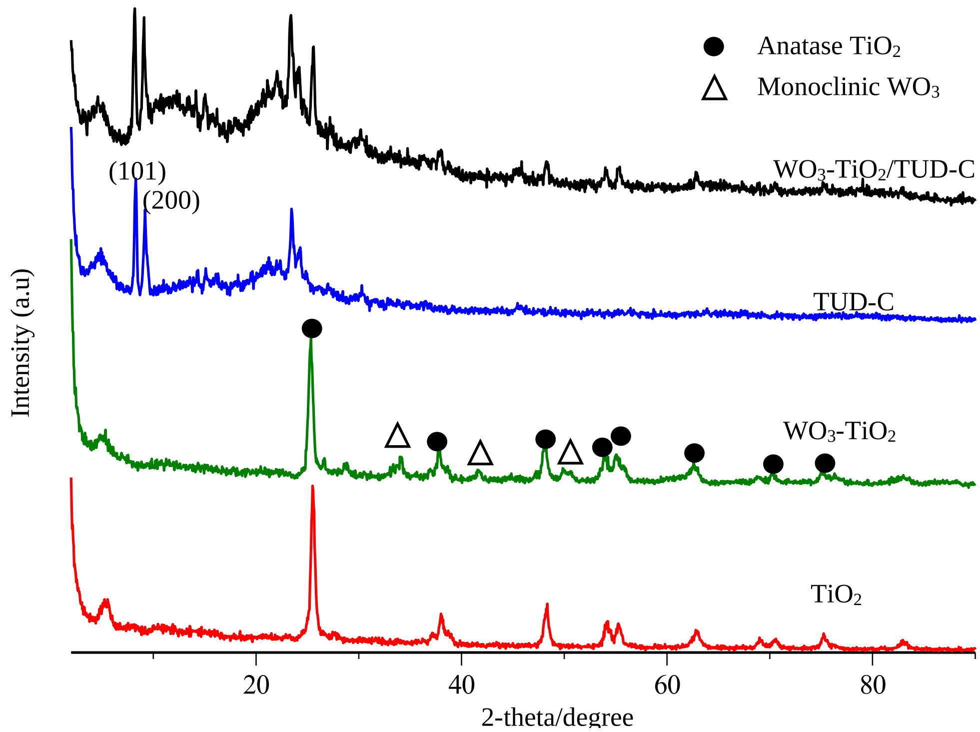

Figure 1. XRD spectra of TiO_2, TUD-C, WO_3-TiO_2, and WO_3-TiO_2/TUD-C

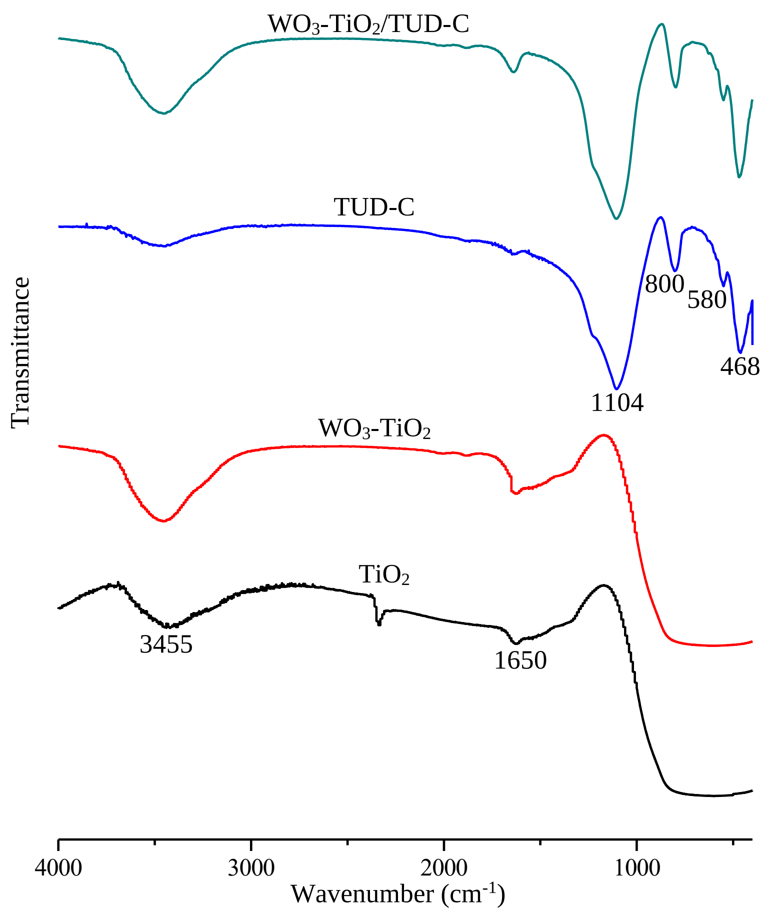

Figure 2. FT-IR spectra of TiO_2, TUD-C, WO_3-TiO_2, and WO_3-TiO_2/TUD-C

Figure 2 shows the FT-IR spectra of TiO_2, WO_3-TiO_2, TUD-C, and WO_3-TiO_2/TUD-C. TiO_2 showed a weak and broad peak at the region between 400 and 800 cm^{-1} relevant to bulk titania skeletal. WO_3-TiO_2/TUD-C showed two peaks at 3455 and 1650 cm^{-1} which were O–H stretching vibration because of the –OH group arising out of hydrolysis which occurred in the sol-gel method. Furthermore, WO_3-TiO_2/TUD-C exhibited some symbolic peaks related to zeolitic ZSM-5 including 468, 550, 800, and 1104 cm^{-1} which corresponded to T–O bend (T = Si or Al atom), MFI phase skeletal vibration, Si-O-Si external symmetric stretching, and Si-O-Si internal symmetric stretching, respectively [21]. There were no peaks discovered for W and Ti-W coordination bonds due to the minuscule loading amount of WO_3.

Figure 3 shows the Diffuse Reflectance UV-Vis (DRUV-Vis) spectra of the pure TiO_2, WO_3-TiO_2, and WO_3-TiO_2/TUD-C. TiO_2 showed a weak absorption peak at 220 nm and an intense absorption peak in the range of 260-320 nm which were attributed to tetrahedral and octahedral Ti or polytitanate $(Ti\text{-}O\text{-}Ti)_n$, respectively [8,18]. As can be seen, WO_3-TiO_2 and WO_3-TiO_2/TUD-C exhibited a notable shift from the region around 200-300 nm to 300-400 nm. The shifting would imply successful loading of WO_3 in the samples. It was reported that WO_3 doped on TiO_2 would cause transition of charge-transfer occurring between the valence and conduction band of TiO_2 as well as the d-orbital of WO_3 [22]. TUD-C showed significant extended absorption range to 450 nm, suggesting incorporation of WO_3-TiO_2 into TUD-C in the material. The result was further supported by the XRD and FTIR analyses as presented above. It is noteworthy that WO_3-TiO_2/TUD-C showed an increment in intensity for the absorption peak at 230 nm which was attributed to the hydrated tetrahedrally coordinated Ti species. The analysis results strongly suggested the formation of more tetrahedrally coordinated Ti species with the presence of TUD-C.

2. Catalytic Oxidation of Cyclohexane

Catalytic oxidation of the materials was assessed through the catalytic oxidation of cyclohexane in the presence of H_2O_2. The catalytic performance of TiO_2 in oxidation of cyclohexane was the lowest, which was 9.2%. It may be due to the low surface area of TiO_2 (20 m^2/g) due to possible agglomeration and aggregation of TiO_2. The catalytic performance of WO_3-TiO_2 in cyclohexane oxidation was 15.8%. It was documented that both WO_3 dopant and TiO_2 could provide oxidative active sites for the cyclohexane oxidation [24]. Even though TUD-C is a zeolitic material which possesses acidity active sites [20], its catalytic performance was lower than that of WO_3-TiO_2, implying the amount of oxidative sites in TUD-C was insufficient.

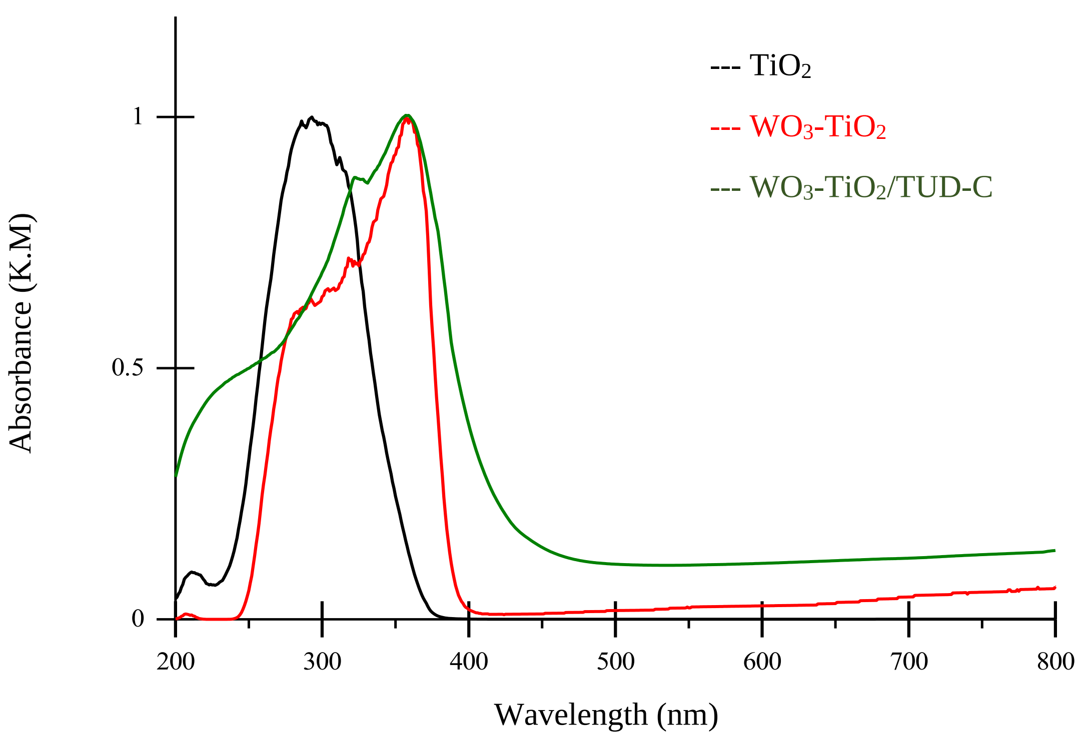

Figure 3. DRUV-Vis spectra of TiO_2, WO_3-TiO_2 and WO_3-TiO_2/TUD-C

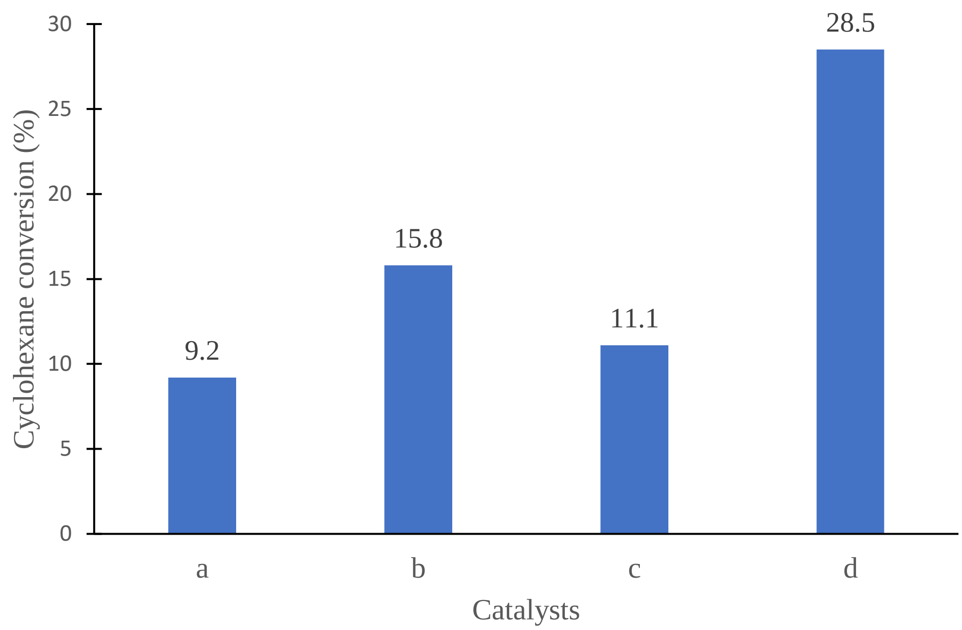

Figure 4. Cyclohexane oxidation percentage of (a) TiO_2, (b) WO_3-TiO_2, (c) TUD-C, and (d) WO_3-TiO_2/TUD-C

From Figure 4, it can be noticed that the catalytic oxidation activity of WO_3-TiO_2/TUD-C was the highest compared to TUD-C, TiO_2, and WO_3-TiO_2. The catalytic performance of WO_3-TiO_2//TUD-C in cyclohexane oxidation was the highest which was 28.5% cyclohexane conversion after 4 h reaction. As observed, catalytic performance of WO_3-TiO_2/TUD-C was 2-fold better than that of WO_3-TiO_2, strongly indicating TUD-C played an important role as support material in the newly designed catalyst. This was due to large surface area of WO_3-TiO_2/TUD-C (83.6 m^2/g) which could facilitate the cyclohexane oxidation. It has been widely accepted that the large surface area could increase the absorptivity and diffusivity of the reactants, leading to enhanced catalytic activity. Besides, the high surface area could allow better dispersion of the active sites of WO_3-TiO_2 onto the TUD-C materials, hence reducing agglomeration and facilitating the accessibility to the active sites of WO_3-TiO_2 [25]. On the other hand, the higher crystallinity degree of WO_3-TiO_2/TUD-C as compared to TUD-C may enhanced the catalytic performance of WO_3-TiO_2/TUD-C. It was reported previously that higher crystallinity may lead to minor defect sites and thus increasing the catalytic efficiency of the material [26].

The attainment of MFI zeolitic-like mesoporous structure in WO_3-TiO_2/TUD-C could contribute to sufficient acidity active sites for the catalytic oxidation of cyclohexane [21]. In addition, the substantial surface area and high crystallinity of WO_3-TiO_2/TUD-C boosted the catalytic efficiency towards cyclohexane oxidation due to the increase of diffusivity and active sites accessibility of the material [20]. Since tetrahedrally coordinated Ti species were claimed as important oxidative active sites [25], the existence of more tetrahedrally coordinated Ti species in WO_3-TiO_2/TUD-C could also be one of the key factors for its enhanced catalytic activity. It could be concluded that the co-existence of WO_3-TiO_2 and TUD-C has brought synergistic effect.

CONCLUSION

A new oxidative catalyst of WO_3-TiO_2 supported on TUD-C was successfully synthesized via combination of sol-gel, wet-impregnation and hydrothermal methods. The prepared WO_3-TiO_2/TUD-C possessed crystalline MFI zeolitic framework. Both the surface area and pore volume of WO_3-TiO_2/TUD-C were higher than that of unsupported WO_3-TiO_2. Besides, usage of TUD-C support caused the formation of more tetrahedrally coordinated Ti species formed in WO_3-TiO_2/TUD-C. It has been demonstrated that WO_3-TiO_2/TUD-C is a promising oxidative catalyst as its catalytic performance in cyclohexane oxidation was two times higher than that of unsupported WO_3-TiO_2.

ACKNOWLEDGEMENTS

Authors are grateful to the financial support from Ministry of Higher Education Malaysia (MOHE) and Universiti Teknologi Malaysia through Fundamental Research Grant Scheme (R.J130000.7854.5F238).

REFERENCES

1. Campbell, M. L. (2011) Cyclohexane. Ullmann's Encyclopedia of Industrial Chemistry. **41**–**47**.

2. Dada, E.A., Achenie, L. (2012) Production of Cyclohexane from Hydrogenation of Benzene using Microreactor Technology. *Computer Aided Chemical Engineering*, **31**, 240–244.

3. Trakarnpruk, W. (2015) Heterogeneous Catalytic Oxidation of Cyclohexane with H_2O_2 Catalyzed by Cs- and TBA-salts of Cu- and Mn-Polyoxotungstates on MCM-41. *International Journal of Chemical Engineering and Applications*, **6(2)**, 120–124.

4. Nina Perkas, N., Wang, Y., Koltypin, Y., Gedanken, A., Chandrasekaran, S. (2001) Mesoporous iron–titania catalyst for cyclohexane oxidation. *Chem. Commun*., 988–989.

5. Xu, L-X., He, C-H., Zhu, M-Q., Wu, K-J., La, Y-L. (2007) Silica-Supported Gold Catalyst Modified by Doping with Titania for Cyclohexane Oxidation. *Catal Lett*., **118**, 248–253.

6. Yao, W., Fang, H., Ou, E., Wang, J., Yan, Z. (2006) Highly efficient catalytic oxidation of cyclohexane over cobalt-doped mesoporous titania with anatase crystalline structure. *Catalysis Communications*, **7(6)**, 387–390.

7. Koh, P. W., Yuliati, L., Lee, S. L. (2019) Kinetics and Optimization Studies of Photocatalytic Degradation of Methylene Blue over Cr-Doped TiO_2 using Response Surface Methodology. *Iranian Journal of Science and Technology, Transactions A: Science*, **43**, 95–103.

8. Koh, P. W., Hatta, M. H. M., Ong, S. T., Yuliati, L., Lee, S. L. (2017) Photocatalytic degradation of photosensitizing and non-photosensitizing dyes over chromium doped titania photocatalysts under visible light. *Journal of Photochemistry & Photobiology, A: Chemistry*, **332**, 215–223.

9. Khaw, S. P., Ooi, Y. K., Lee, S. L. (2016) Vanadium oxides doped porous titania photocatalysts for phenol photodegradation. *Malaysian Journal of Fundamental and Applied Sciences*, **12(1)**, 28–33.

10. Ekhsan, J. M., Lee, S. L., Nur, H. (2014) Niobium oxide and phosphoric acid impregnated silica-titania as oxidative-acidic bifunctional catalyst. *Applied Catalysis A: General*, **471**, 142–148.

11. Dunn, J. P., Stenger, H. G., Wachs, I. E. (1999) Oxidation of SO_2 over Supported Metal Oxide Catalysts. *Journal of Catalysis*, **181**, 233–243.

12. Wang, J., Sun, W., Zhang, Z., Jiang, Z., Wang, X., Xu, R., Zhang, X. (2008) Preparation of Fe-doped mixed crystal TiO_2 catalyst and investigation of its sonocatalytic activity during degradation of azo fuchsine under ultrasonic irradiation. *Journal of Colloid and Interface Science*, **320(1)**, 202–209.

13. Pourdayhimi, P., Koh, P. W., Nur, H., Lee, S. L. (2019) Highly Crystalline Zinc Oxide/Mesoporous Hollow Silica Composites Synthesized at Low Temperature for the Photocatalytic Degradation of Sodium Dodecylbenzenesulfonate. *Australian Journal of Chemistry*, **72(4)**, 252–259.

14. Lee, S. L., Wei, S. C., Nur, H., Hamdan, H. (2010) Enhancement of Brønsted Acidity in Sulfate-Vanadium Treated Silica-Titania Aerogel as Oxidative-Acidic Bifunctional Catalyst. *International Journal of Chemical Reactor Engineering*, **8**, 63.

15. Hamdy, M. S., & Mul, G. (2013) TUD-1-encapsulated HY zeolite: A new hierarchical microporous/mesoporous composite with extraordinary performance in benzylation reactions. *ChemCatChem*, **5(10)**, 3156–3163.

16. Quek, X. Y., Liu, D., Cheo, W. N. E., Wang, H., Chen, Y., & Yang, Y. (2010) Nickel-grafted TUD-1 mesoporous catalysts for carbon dioxide reforming of methane. *Applied Catalysis B: Environmental*, **95(3–4)**, 374–382.

17. Ooi, Y. K., Yuliati, L, Lee, S. L. (2016) Phenol photocatalytic degradation over mesoporous TUD-1-supported chromium oxide-doped titania photocatalyst. *Cuihua Xuebao/Chinese Journal of Catalysis*, **37(11)**, 1871–1881.

18. Sha'ri @ Shangari, F., Lee, S. L. (2017) Synthesis and characterization of TUD-C impregnated with zinc oxide. *eProceedings Chemistry*, **2**, 169–178.

19. Yao, W., Chen, Y., Min, L., Fang, H., Yan, Z., Wang, H., Wang, J. (2006) Liquid oxidation of cyclohexane to cyclohexanol over cerium-doped MCM-41. *Journal of Molecular Catalysis A: Chemical*, **246(1-2)**, 162–166.

20. Ooi, Y. K., Yuliati, L., Hartanto, D., Nur, H., Lee, S. L. (2016) Mesostructured TUD-C supported molybdena doped titania as high selective oxidative catalyst for olefins epoxidation at ambient condition. *Microporous and Mesoporous Materials*, **225**, 411–420.

21. Ooi, Y. K., Hussin, F., Yuliati, L., Lee, S. L. (2019) Comparison study on Molybdena-Titania supported on TUD-1 and TUD-C synthesized via sol-gel templating method: Properties and catalytic performance in olefins epoxidation. *Materials Research Express*, **6**, 074001.

22. Zangeneh, H., Zinatizadeh, A. A. L., Habibi, M., Akia, M., Hasnain Isa, M. (2015) Photocatalytic oxidation of organic dyes and pollutants in wastewater using different modified titanium dioxides: A comparative review. *Journal of Industrial and Engineering Chemistry*, **26(2015)**, 1–36.

23. Pal, B., Vijayan, B. L., Krishnan, S. G., Harilal, M., Basirun, W. J., Lowe, A., Yusoff, M. M., Jose, R. (2018) Hydrothermal syntheses of tungsten doped TiO_2 and TiO_2/WO_3 composite using metal oxide precursors for charge storage applications. *Journal of Alloys and Compounds*, **740**, 703–710.

24. Leung, K, Nielsen, I. M. B., Criscenti, L. J. (2009) Elucidating the Bimodal Acid-base Behavior of the Water-silica Interface from first Principles. *Journal of the American Chemical Society*, **131**, 18358–18365.

25. Lee, S. L., Hamdan, H. (2008) Sulfated Silica-Titania Aerogel as A Bifunctional Oxidative and Acidic Catalyst in the Synthesis of Diols. *Journal of Non-Crystalline Solids*, **354(33)**, 3939–3943.

26. Siah, W. R., Lintang, H. O., Shamsuddin, M., Yuliati, L. (2016) High photocatalytic activity of mixed anatase-rutile phases on commercial TiO_2 nanoparticles. *IOP Conf. Series: Materials Science and Engineering*, **107**, 012005.